42nd AIAA Aerospace Sciences Meeting and Exhibit
5 - 8 January 2004, Reno, Nevada

AIAA 2004-1129

Modeling the effect of shock unsteadiness in shock-wave/ turbulent boundary layer interactions

Krishnendu Sinha*, Krishnan Mahesh† and Graham V. Candler‡
Aerospace Engineering and Mechanics & Army HPC Research Center
University of Minnesota, Minneapolis, MN 55455

Abstract

Reynolds averaged Navier-Stokes methods often cannot predict shock/turbulence interaction correctly. This may be because RANS models do not account for the unsteady motion of the shock wave that is inherent in these interactions. Sinha *et al.* [*Phys. Fluids*, Vol. 15, No. 8 (2003)] propose a shock-unsteadiness correction that significantly improves turbulence prediction across a normal shock in a uniform mean flow. In this paper, we generalize the modification to simulate complex flows using k-ϵ, k-ω, and Spalart-Allmaras models. In compression-corner flows, the corrected k-ϵ and k-ω models amplify the turbulent kinetic energy less through the shock compared to the standard models. This results in improved prediction of the separation shock location, a delayed reattachment, and a slower recovery of the boundary layer on the ramp. In the Spalart-Allmaras model, the modification amplifies eddy viscosity across the shock, moving the separation location closer to the experiment.

Introduction

The characteristics of a turbulent boundary layer in a supersonic flow can be drastically altered by a shock wave. The interaction can lead to high pressure and heating loads as well as regions of separated flow. These play an important role in the design and operation of high-speed aerospace vehicles and propulsion systems. Commonly studied flow configurations include compression ramps, oblique shocks impinging on boundary layers, transonic airfoils, and single or double fins on plates.

Engineering prediction of shock-wave / turbulent boundary layer interaction relies on Reynolds averaged Navier-Stokes (RANS) simulations. However, significant disagreement with experimental data is observed, especially in the presence of strong shock waves.[1,2] In compression corner flows with high deflection angle, for example, the method cannot predict the location of the separation shock, the size of the separation region at the corner, and the mean velocity profiles downstream of the interaction.[2,3] This may be due to the high degree of compressibility and rapid strain rates associated with a shock wave. Conventional turbulence models do not account for these effects, and therefore yield significant error. Several modifications have been proposed to improve the predictions, e.g. realizability constraint,[2] compressibility correction,[3,4] length-scale modification[4] and rapid compression correction.[4] The outcome of the modifications vary from model to model and also with test conditions.

The flow field generated by the interaction of shock wave with a turbulent boundary layer is inherently unsteady. As pointed out by Dolling,[5] some knowledge of the unsteadiness is essential to predict the magnitude and distribution of the mean flow properties. Turbulence models used in RANS methods do not account for the unsteady motion of the shock. This is identified as one of the main reasons for their poor performance in strong shock-wave/turbulent boundary layer interactions.[6] Therefore, the effect of the shock unsteadiness needs to be included in RANS simulations.

Sinha *et al.*[7] study the interaction of homogeneous isotropic turbulence with a normal shock in the RANS framework. They show that standard k-ϵ model[8] with compressibility corrections[9,10] over-predicts the turbulent kinetic energy, k, behind the shock. Eddy viscosity corrections based on the realizability constraint are shown to improve results, but still do not correctly predict k behind the shock. Sinha *et al.*[7] identify a damping mechanism caused by the coupling between shock motion and turbulent fluctuations in the incoming flow. They propose a model for this shock-unsteadiness effect based on an analysis of the linearized conservation equations that govern shock/homogeneous turbulence interaction. The model is shown to predict the evolution of turbulent kinetic energy across the shock accurately. However, it is strictly applicable only when the mean flow on

*Postdoctoral Associate, Member AIAA
†Assistant Professor, Member AIAA
‡ Professor, Associate Fellow AIAA

either side of the shock is uniform. The current paper generalizes the shock-unsteadiness model presented by Sinha *et al.*[7] to flows with additional mean gradients. It is then applied to interaction of turbulent boundary layers with shock waves.

The paper is organized as follows. We start with a brief description of the governing equations, and the k-ϵ , k-ω and Spalart-Allmaras (SA) turbulence models. The shock-unsteadiness correction proposed by Sinha *et al.*[7] and its implementation is discussed in detail. Next, the numerical method used to solve the conservation equations is presented along with the boundary conditions used in the simulations. This is followed by the results obtained for the compression corner flows. Ramp angles of 24°, 20° and 16° are considered, and the model predictions are compared to experimental data of Settles and Dodson.[11]

Simulation methodology

We solve the two-dimensional Favre-averaged Navier-Stokes equations for the mean flow, as presented in Ref. 12. The k-ω model of Wilcox,[13] the low Reynolds number k-ϵ model of Launder and Sharma,[8] and the Spalart-Allmaras model are used for turbulence closure. The modeled transport equations for the turbulent kinetic energy, the turbulent dissipation rate ϵ, and the specific dissipation rate ω are given in Refs. 8 and 13. The Spalart-Allmaras model[14] solves a transport equation for $\bar{\rho}\tilde{\nu}$, where $\bar{\rho}$ is the mean density and $\tilde{\nu}$ is identical to the turbulent eddy viscosity, ν_T, except in the viscous sub-layer and the buffer region close to a solid boundary.

Shock-unsteadiness modification to the k-ϵ and k-ω models

Sinha *et al.*[7] applied the k-ϵ model to the interaction of homogeneous isotropic turbulence with a normal shock wave. They showed that the model excessively amplifies the turbulent kinetic energy through the shock. This is due to the fact that the production of k, given by

$$P_k = \mu_T(2S_{ij}S_{ji} - \tfrac{2}{3}S_{ii}^2) - \tfrac{2}{3}\bar{\rho}kS_{ii} \qquad (1)$$

is proportional to S_{ii}^2, which is very large in magnitude in the region of the shock. The production of k in the k-ω model is identical to (1), and therefore it also overly amplifies k across the shock. Here, $S_{ij} = \frac{1}{2}(\partial\tilde{u}_i/\partial x_j + \partial\tilde{u}_j/\partial x_i)$ is the symmetric part of the strain rate tensor and $\tilde{u}_i$ is the component of the Favre-averaged velocity in the x_i direction. The turbulent eddy viscosity μ_T is given by $\mu_T = \bar{\rho}k/\omega$ in the k-ω model, and $\mu_T = c_\mu f_\mu \bar{\rho}k^2/\epsilon$ in the k-ϵ formulation, where $c_\mu = 0.09$ and $f_\mu = \exp(-3.4/(1. + 0.02Re_t)^2)$ is a damping function. Here, $Re_t = \bar{\rho}k^2/\mu\epsilon$ is the turbulent Reynolds number and μ is the molecular viscosity of the fluid.

Sinha *et al.*[7] argue that the eddy viscosity assumption breaks down in the highly non-equilibrium flow thfough a shock, and a more accurate amplification of k is obtained by setting $\mu_T = 0$ in Eq. (1). They also note that unsteady shock motion damps the amplification of k across a shock. Based on linear analysis results, they propose the following modification to the production term in a shock wave,

$$P_k = -\tfrac{2}{3}\bar{\rho}kS_{ii}\ (1 - b_1') \qquad (2)$$

where

$$b_1' = 0.4\left(1 - e^{1-M_{1n}}\right) \qquad (3)$$

represents the damping effect caused by the coupling between the shock unsteadiness and the upstream velocity fluctuations. Here, M_{1n} is the upstream Mach number normal to the shock. The above model is shown to accurately predict the amplification of k in shock/homogeneous turbulence interactions.[7]

The amount of turbulence in a boundary layer directly affects flow separation in adverse pressure gradient. Higher turbulence levels delay separation, which may explain why simulations using k-ω and k-ϵ models predict later separation than what is observed in experiments.[2,15] Lower production of k in the shock due to shock-unsteadiness effect is therefore expected to improve results. In order to match the production of k in the shock to the value prescribed by Eq. (2), we replace μ_T in Eq. (1) by $c_\mu'\ \mu_T$ where

$$c_\mu' = 1 - f_s\left[1 + \frac{b_1'/\sqrt{3}}{s}\right] \qquad (4)$$

for the k-ω model. Here $s = S/\omega$ is a dimensionless mean strain rate, and $S = \sqrt{2S_{ij}S_{ji} - \frac{2}{3}S_{ii}^2}$. For the k-ϵ model,

$$c_\mu' = 1 - f_s\left[1 + \frac{b_1'/\sqrt{3}}{sc_\mu f_\mu}\right] \qquad (5)$$

where $s = Sk/\tilde{\epsilon}$ and $\tilde{\epsilon} = \epsilon + 2\nu(\partial\sqrt{k}/\partial x_j)^2$ is the total dissipation rate obtained by adding the low Reynolds number term in the k-equation to the turbulent dissipation rate.[8] The function f_s identifies the region of the shock wave in terms of the ratio S_{ii}/S.

$$f_s = \tfrac{1}{2} - \tfrac{1}{2}\tanh(5S_{ii}/S + 3) \qquad (6)$$

such that $f_s = 1$ in regions of high compression and $f_s = 0$ otherwise. Note that the exact form of f_s was obtained by trial and error.

Shock-unsteadiness modification to SA model

In the Spalart-Allmaras model, the mean flow influences the turbulence field via the production term that is a function of the mean vorticity. Therefore, the eddy viscosity is insensitive to mean dilatation in a shock wave. However, the mean vorticity field in a turbulent boundary layer changes across a shock wave. This can alter the production term, and thus can change $\tilde{\nu}$ in the vicinity of the shock. In a 24° compression corner flow, for example, the interaction of a turbulent boundary layer with an oblique shock results in a small increase in $\tilde{\nu}$ (less than 5% of the local $\tilde{\nu}$ magnitude).

Interaction with a shock wave enhances the turbulent fluctuations in a flow. Sinha *et al.*[7] propose the following model for the amplification of k and ϵ across a shock wave.

$$\frac{k_2}{k_1} = \left(\frac{\tilde{u}_{n,1}}{\tilde{u}_{n,2}}\right)^{\frac{2}{3}(1-b_1')} \quad \text{and} \quad \frac{\epsilon_2}{\epsilon_1} = \left(\frac{\tilde{u}_{n,1}}{\tilde{u}_{n,2}}\right)^{\frac{2}{3}c_{\epsilon 1}}$$

where subscripts 1 and 2 refer to the locations upstream and downstream of the shock, respectively, and $\tilde{u}_n$ is the mean velocity component normal to the shock. b_1' represents the effect of the shock-unsteadiness, given by (3), and $c_{\epsilon 1} = 1.25 + 0.2(M_{1n} - 1)$. Noting that $\nu_T \propto k^2/\epsilon$, the change in ν_T or $\tilde{\nu}$ across a shock can be estimated as

$$\frac{\tilde{\nu}_2}{\tilde{\nu}_1} = \left(\frac{k_2}{k_1}\right)^2 \frac{\epsilon_1}{\epsilon_2} = \left(\frac{\tilde{u}_1}{\tilde{u}_2}\right)^{c_{b1}'}$$

where $c_{b1}' = \frac{4}{3}(1 - b_1') - \frac{2}{3}c_{\epsilon 1}$. This can be achieved by a production term of the form $-c_{b1}'\bar{\rho}\tilde{\nu}S_{ii}$ in the transport equation for $\bar{\rho}\tilde{\nu}$. Note that this additional term is effective only in regions of strong compression, and therefore does not alter the standard Spalart-Allmaras model elsewhere.

Numerical method

The governing equations are discretized in a finite volume formulation where the inviscid fluxes are computed using a modified form of the Steger-Warming flux splitting approach.[16] The turbulence model equations are fully coupled to the mean flow equations. The details of the formulation are given in Ref. 17. The method is second order accurate both in stream-wise and wall normal directions. The viscous fluxes and the turbulent source terms are evaluated using second order accurate central difference methods. The implicit Data Parallel Line Relaxation method of Wright *et al.*[18] is used to obtain steady-state solutions.

Boundary conditions

Inlet profiles for the computations are obtained from separate flat plate simulations using the standard k-ω , k-ϵ and SA models discussed above. The value of the momentum thickness reported in the experiments[11] is matched to obtain the mean flow and turbulence profiles at the inlet boundary of the compression ramp simulations.

Nominal test section conditions reported in the experiments are specified in the free stream, and no-slip isothermal boundary condition (based on wall temperature measurements) is applied on solid walls. For the turbulence model equations, the boundary conditions at the wall are $k = 0$, $\epsilon = 0$, $\tilde{\nu} = 0$ and $\omega = 60\nu_w/\beta\Delta y_1^2$, where ν_w is the kinematic viscosity at the wall, $\beta = 3/40$ is a model constant and Δy_1 is the distance to the next point away from the wall. Following Menter,[19] the free stream conditions used for the flat plate simulations with the k-ω model are

$$\omega_\infty = 10\ U_\infty/L\,, \quad k_\infty = 0.01\ \nu_\infty\omega_\infty$$

where $L = 1$ m is a characteristic length of the plate and the subscript ∞ denotes the freestream conditions. In case of the k-ϵ model,

$$k_\infty = 0.002\ U_\infty^2\,, \quad \epsilon_\infty = 0.1\ c_\mu\rho_\infty k_\infty^2/\mu_\infty$$

are used in the freestream. For the compression ramp simulations, k, ϵ and ω values at the boundary layer edge in the inlet profile are prescribed as the free stream conditions at the top boundary. A supersonic extrapolation is used at the exit boundary of the domain.

Simulation Results

We compute the three compression ramp flows listed in Table I. The standard k-ω , k-ϵ and SA models as well as the models with the shock-unsteadiness modification are used in the simulations. Experimental measurement of surface pressure, skin friction coefficient and mean velocity profiles at several streamwise locations in these flows are presented by Settles and Dodson.[11] The standard k-ω and k-ϵ model results show similar trends, and the effect of the shock-unsteadiness correction is comparable in these two models. Therefore, the simulations using the k-ω and k-ϵ model are described first. This is followed by the SA model results.

Ramp angle	24°	20°	16°
Mach number	2.84	2.80	2.85
Freestream temperature (K)	100.3	102.3	102.1
Freestream density (kg/m^3)	0.83	0.88	0.82
Freestream velocity (m/s)	570	568	578
Wall temperature (K)	276.1	273.9	282.0
Boundary layer thickness (m)	0.024	0.025	0.026
Momentum thickness (m)	0.0012	0.0013	0.0013

Table I. Free stream conditions and characteristics of the incoming turbulent boundary for the compression ramp flows.

24° compression ramp

In the 24° compression corner simulations, the computational domain consists of a 10 cm flat plate followed by a 15 cm long ramp, and extends to 5 cm above the plate at the inlet location. The grid consists of 120 equispaced points in the stream-wise direction and 100 exponentially stretched points in the wall normal direction. The first point is located 0.002 mm from the wall which is equivalent to 0.6 wall units or less along the solid wall. This grid is found to be sufficient to obtain grid independent solutions.

The surface pressure distribution and the skin friction coefficient c_f computed using the standard k-ω and k-ϵ models is shown in Fig. 1. Experimental data[11] are also plotted for comparison. The streamwise distance s along the plate and the ramp is normalized by the incoming boundary layer thickness δ_0, where $s = 0$ represents the corner. The model results are similar to those reported in literature.[2,15] Both models predict the separation shock location downstream of the experiment. The k-ω model matches the pressure plateau in the separation region, whereas the k-ϵ model overpredicts it by about 15%. The subsequent pressure rise on the ramp is also overpredicted by both models. The skin friction plot shows that the models predict a later separation than the experiment. The reattachment location is also downstream of the experimental data. The k-ϵ model greatly overpredicts c_f on the ramp, whereas the k-ω model yields good agreement with the measurements downstream of reattachment.

Next, we apply the shock-unsteadiness correction to this flow. The modification is effective only in the separation shock as identified by $S_{ii}/S < -0.3$ (see Fig. 2). In the region of the shock wave that penetrates the incoming boundary layer ($y < \delta_0$), the Mach number normal to the shock varies between 1.2

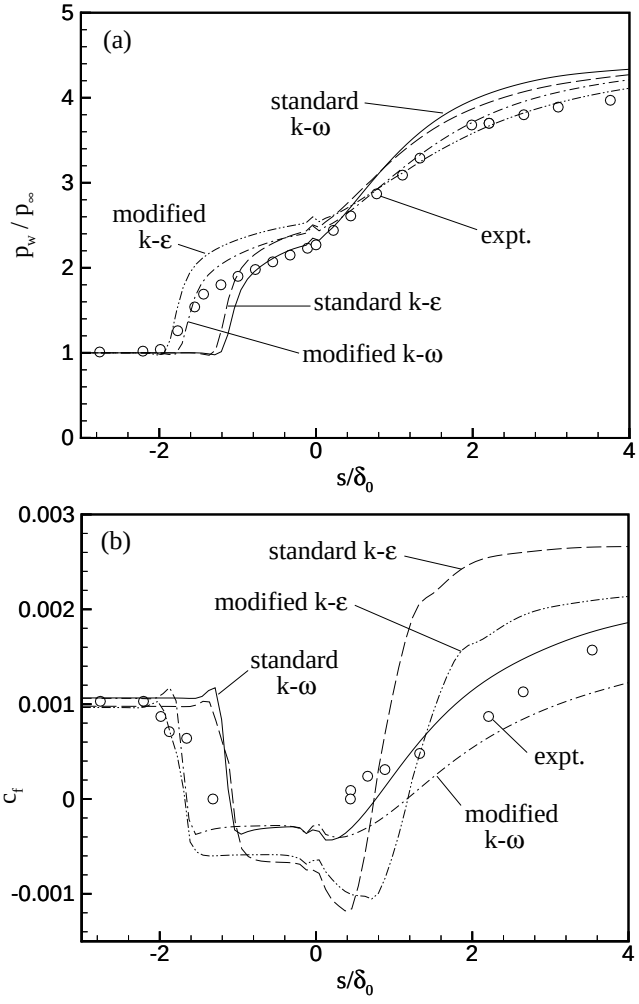

Figure 1. Variation of (a) normalized surface pressure, and (b) skin friction coefficient along a 24° compression corner obtained using the standard and modified k-ω and k-ϵ models.

and 1.6. $M_{1n} \simeq 1.2$ close to the wall and it attains higher values at the boundary layer edge. The local value of M_{1n} is used to evaluate the damping parameter b_1' at each point in the shock. Note that M_{1n} is computed by taking a dot product of the streamwise Mach number in the incoming boundary layer with the pressure gradient vector in the shock wave. Figure 3 shows the variation of k along a streamline originating at $y/\delta_0 = 0.2$ in the incoming boundary layer. The turbulent kinetic energy is normalized by its value upstream of the separation location. The standard k-ω model amplifies k by a factor of 2.8 across the separation shock (at $x \simeq -0.8\delta_0$) that is followed by further increase in the shear layer enclosing the separated flow region at the corner. The highest value of k is attained in the reattachment region and k decreases as the boundary layer recovers to an equilibrium state on the ramp. Using the shock-

unsteadiness correction in the k-ω model we get a much smaller increase in k across the separation shock at $x \simeq -1.5\delta_0$. This is because of the lower production of turbulence caused by the shock-unsteadiness correction. The modification reduces P_k by up to 80% of the value predicted by the original k-ω model. Also, note that the shock-unsteadiness modification is applied only in the region of the shock wave as identified in Fig. 2, and its effect on k is localized to this region. The variation of k downstream of the shock is similar in both the standard and modified k-ω models. Applying the shock-unsteadiness modification in the k-ϵ model yields lower amplification of k across the shock similar to that shown in Fig. 3.

A lower amplification of k across the shock caused by the shock-unsteadiness modification moves the separation point upstream and the model predictions match the experimental location of the pressure rise well (see Fig. 1(a)). The modification results in a higher pressure plateau than the corresponding standard model, and reproduces the experimental pressure rise on the ramp accurately. The drop in c_f at $s \simeq -2\delta_0$ as predicted by the modified k-ω and k-ϵ models (see Fig. 1(b)) agree well with the experimental measurements, but the size of the separation region is overpredicted. Finally, the modification yields a lower c_f on the ramp as compared to the standard models.

The mean velocity profiles at different streamwise locations computed using the standard and modified k-ω models are shown in Fig. 4. Both models match the experimental data in the incoming boundary layer at $s/\delta_0 = -2.76$. The shock-unsteadiness correction

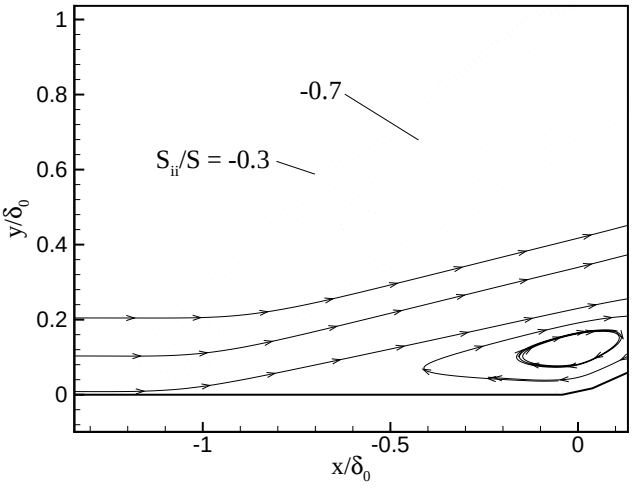

Figure 2. Contours of S_{ii}/S (-0.3,-0.4,...,-0.7) shown by dotted lines and some representative streamlines in the k-ω simulation of a 24° compression ramp flow.

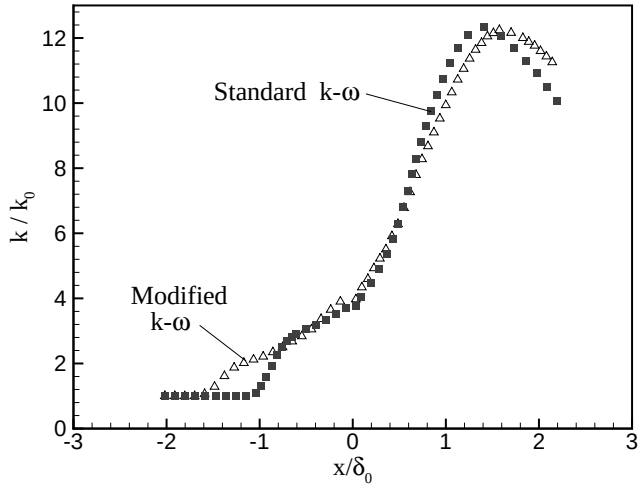

Figure 3. Variation of turbulent kinetic energy along a streamline originating at $y/\delta_0 = 0.2$ in the k-ω simulation of a 24° compression ramp flow.

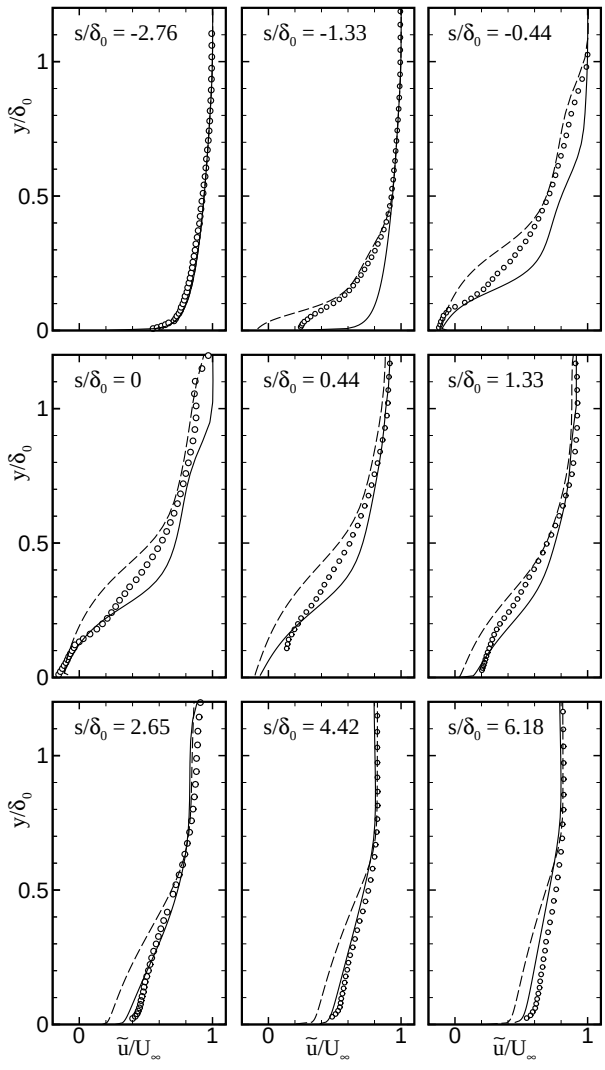

Figure 4. Comparison of mean velocity profiles obtained using the standard k-ω model (——) and the shock-unsteadiness modification (− − −) with experimental data (○) in a 24° compression ramp flow.

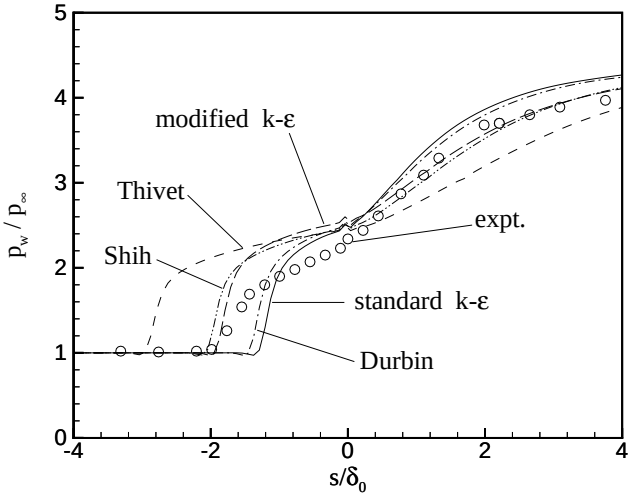

Figure 5. Normalized surface pressure distribution in the 24° compression-corner flow as computed by the standard k-ϵ model and different realizable k-ϵ models.

results in better prediction of the velocity profiles near the separation location than the original k-ω model. Most notably, the outer part of the boundary layer at $s/\delta_0 = -1.33, -0.44$ and 0 are reproduced well. However, the modification results in a larger recirculation region than the experiment, and therefore predicts lower velocity close to the wall. This also results in a slower recovery of the boundary layer on the ramp as compared to the standard k-ω model. Note that the velocity profiles obtained using the standard and modified k-ϵ models, not shown here, are very similar to those in Fig. 4.

As pointed out earlier, the Mach number normal to the shock varies between 1.2 and 1.6 in the region of the shock that penetrates the boundary layer. Using an average value of $M_{1n} = 1.4$ to evaluate b_1' in the entire region of the shock wave results in identical results to that obtained using the exact variation of M_{1n}. Also, there is very little sensitivity of the simulation results to the value of M_{1n} in this range $(1.2 \leq M_{1n} \leq 1.6)$.

Another way to suppress the amplification of turbulence across the shock is to use the realizability constraint, $0 \leq \widetilde{u_i'' u_i''} \leq 2k$. Different realizable models have been proposed in the literature. Here, we use the models presented by Durbin,[20] Thivet *et al.*[21], and Shih *et al.*[22] to compute the 24° compression-corner flow. The normalized pressure distribution in Fig. 5 shows that all the realizable models yield some improvement over the standard k-ϵ model. However, the results are highly dependent on the specific form of the realizability correction used. Durbin's model[20] moves the separation shock location upstream by a small amount, whereas the model by Thivet *et al.*[21] predicts the shock location upstream of the experimental data. The realizable model by Shih *et al.*[22] is found to match experimental data well (also see Ref. 2) and its prediction is similar to the k-ϵ model with shock-unsteadiness modification. Note that the correction term (2) satisfies the realizability constraint because the normal Reynolds stresses in the shock are modeled as $\frac{2}{3}\bar{\rho}k$ (obtained using $\mu_T = 0$).

20° compression ramp

We next apply the shock-unsteadiness modification to a 20° compression ramp flow. An average value of upstream normal Mach number $M_{1n} = 1.4$ is used to compute the model coefficient b_1' in the region of the shock wave. Based on the results in the 24° case, we do not expect the model predictions to be very sensitive to the value of M_{1n} used in Eq. (3). The simulation results are shown in Figs. 6 and 7 along with experimental data by Settles and Dodson.[11] Note that the computational domain and grid used in this flow are very similar to those in the 24° case.

The location of the separation shock pressure rise as predicted by the standard k-ω and k-ϵ models is much downstream of the experimental data (see Fig. 6(a)). The shock-unsteadiness correction moves the separation shock upstream. The effect of the modification is small in the k-ω simulation whereas the modified k-ϵ model yields a separation shock location that compares much better with the data. Also note that the modified k-ϵ model results in a higher pressure plateau in the separation region that is similar to the 24° case. All the models agree well with the pressure measurements on the ramp.

The skin friction data in Fig. 6(b) follows a pattern similar to that obtained in the 24° ramp flow. The standard k-ω and k-ϵ models predict a smaller separation region than the experiment. By comparison, the shock-unsteadiness modification yields a good agreement with the measured separation location for both the models. However, none of the models match the decrease of c_f on the plate ($s \simeq -0.8\,\delta_0$). The correction also leads to later reattachment and a lower skin friction on the ramp as compared to the standard models. Note that the modified k-ω model matches the experimental skin friction on the ramp up to $s \simeq 2.5\,\delta_0$.

The mean velocity profiles obtained using the standard and modified k-ϵ models are compared with experimental measurements in Fig. 7. The trends are similar to the 24° compression ramp flow presented above. The most significant improvement caused by the shock-unsteadiness modification is in the vicinity

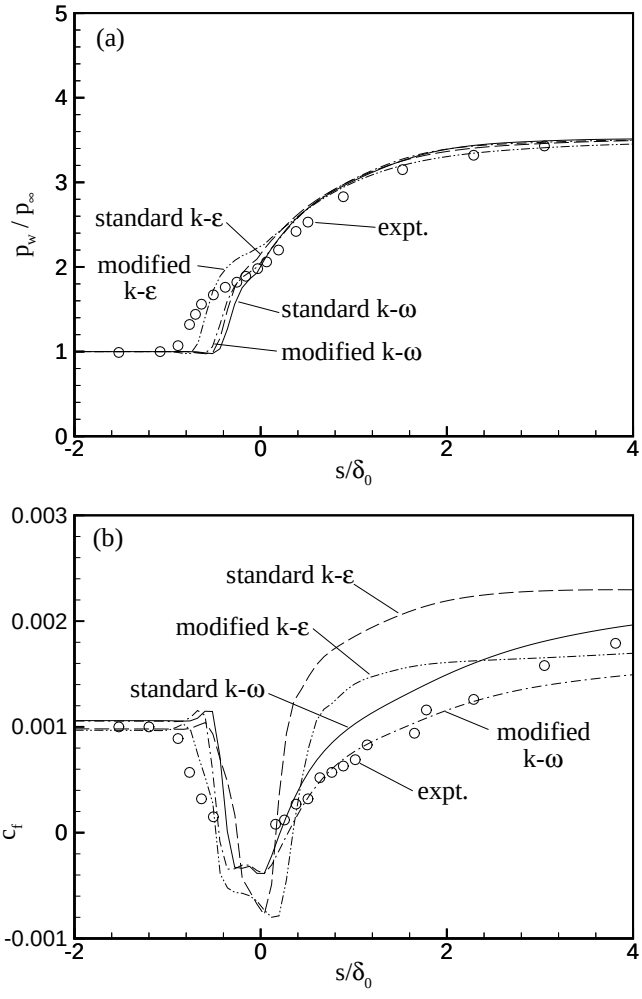

Figure 6. Variation of (a) normalized surface pressure, and (b) skin friction coefficient along a 20° compression corner obtained using the standard and modified k-ω and k-ϵ models.

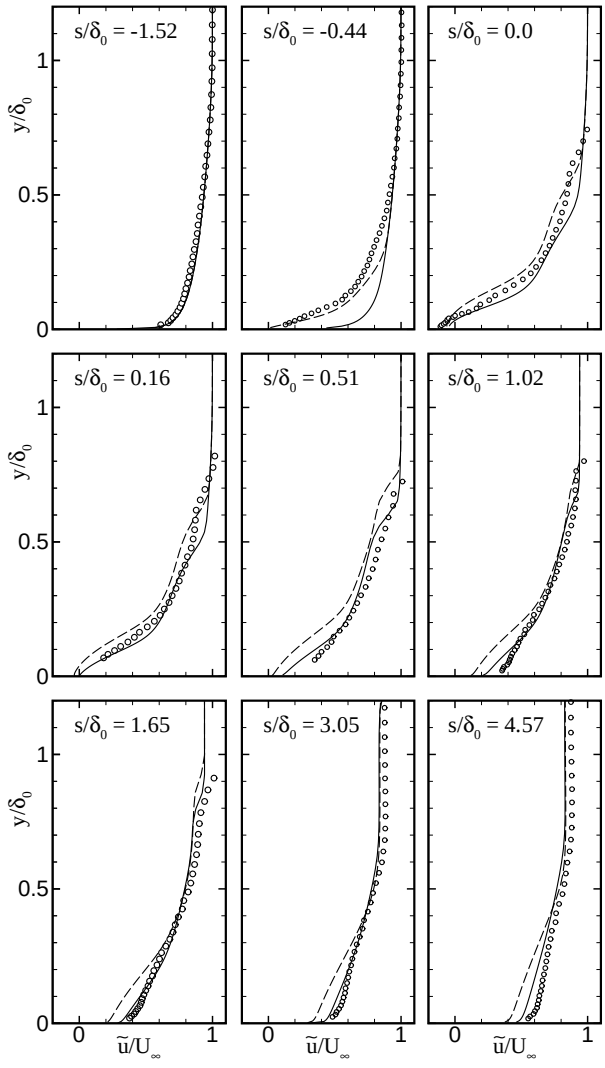

Figure 7. Comparison of mean velocity profiles obtained using the standard k-ϵ model (——) and the shock-unsteadiness modification (− − −) with experimental data (○) in a 20° compression ramp flow.

of the separation point. Specifically, at $s = -0.44\ \delta_0$, an attached boundary layer is obtained using the standard k-ϵ model whereas the modification predicts separated flow that is close to the experimental data. The modified k-ϵ model also reproduces the location of the shock wave well, as seen in the velocity variation in the outer part of the boundary layer at the corner and at $s = 0.16\ \delta_0$. Finally, the correction results in a slower recovery of the boundary layer on the ramp. The k-ω model results, not shown here, are similar to those presented in Fig. 7 but the improvement caused by the shock-unsteadiness modification in the k-ω model is smaller than the k-ϵ results.

16° compression ramp

The flow over a 16° compression ramp is simulated using the standard and modified models, and the results are shown in Figs. 8 and 9. The computational domain and grid used in these simulations are very similar to the 24° case. An exception is the k-ϵ simulation which requires substantially higher resolution at the corner. Streamwise grid spacing of 0.2 mm in this region is used to reproduce a small separation region at the corner. The reference quantities for this test case are listed in Table I. An average value of $M_{1n} = 1.3$ is used in this flow for evaluating the shock-unsteadiness correction.

The flow in this case is near incipient separation, such that the pressure variation (Fig. 8(a)) does not have a distinct pressure plateau that is observed at high ramp angles. All the models reproduce the experimental pressure measurements accurately, which points to the fact that the effect of the shock-unsteadiness correction on the pressure distribution is

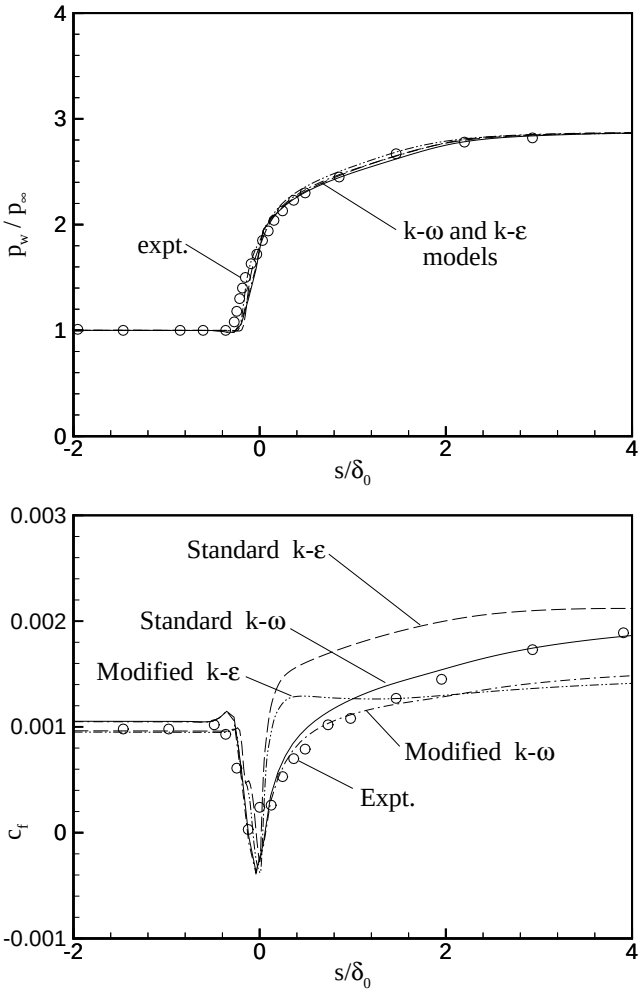

Figure 8. Variation of (a) normalized surface pressure, and (b) skin friction coefficient along a 16° compression corner obtained using the standard and modified k-ω and k-ϵ models.

negligible for small ramp angles. The skin friction coefficient (Fig. 8(b)) shows a small region of separated flow at the corner. The standard and modified models yield almost identical results on the plate ($s < 0$) that agree well with the experimental data. However, the model predictions differ in the recovery region on the ramp. The standard k-ϵ model over-predicts the skin friction whereas the standard k-ω model matches the experimental data. The shock-unsteadiness modification results in lower c_f for both the models. The mean velocity profiles in Fig. 9 show that both the standard and modified k-ϵ models agree well with the experimental data. There is negligible effect of the shock-unsteadiness modification on the k-ϵ results except for the near wall region on the ramp. The modified k-ϵ model yields a less full velocity profile close to the wall than the standard model. The k-ω results show a similar trend.

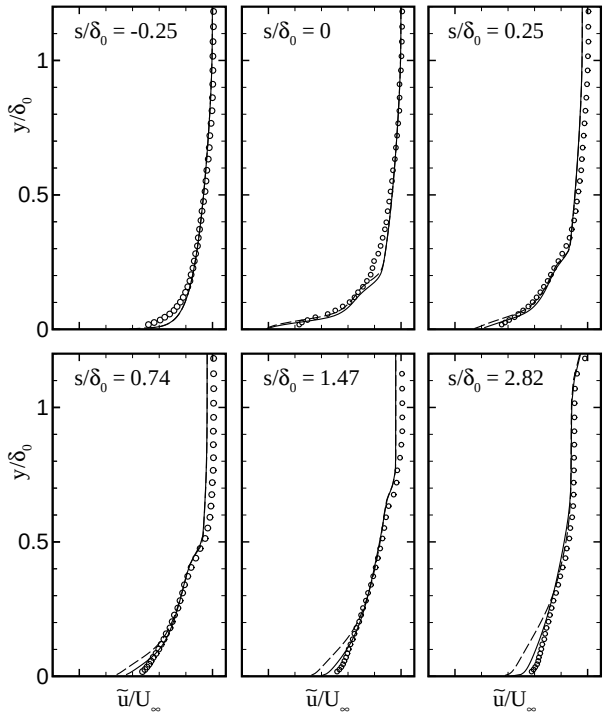

Figure 9. Comparison of mean velocity profiles obtained using the standard k-ϵ model (——) and the shock-unsteadiness modification (− − −) with experimental data (○) in a 16° compression ramp flow.

Spalart-Allmaras model results

The effect of the shock-unsteadiness modification to the Spalart-Allmaras model is tested in a 24° compression corner flow (see Table I). The results are shown in Fig. 10. The standard SA model predicts the separation shock location significantly upstream of the experiment. The pressure plateau is over-predicted and the pressure on the ramp is lower than the experimental data. The skin-friction coefficient drops below the flat plate value of 0.0011 at $s/\delta_0 \simeq -2.7$ that is upstream of the onset of separation in the experiment. The standard SA model also predicts a large separation region and c_f on the ramp is much lower than the experimental measurement. The production due to shock in the SA model results in higher eddy viscosity behind the separation shock compared to the standard model. Note that $M_{1n} = 1.4$ yields $c'_{b1} = 0.27$ in this flow. Higher turbulent viscosity moves the separation point closer to the experiment, but the modification is not enough to match the location of the separation shock. A higher value of $c'_{b1} = 0.7$ gives much better agreement with the experimental pressure measurement, both near the separation location as well as on the ramp. Using $c'_{b1} = 0.7$ also matches the drop in c_f at $s/\delta_0 = -2$. The modification increases c_f on the ramp but the results are significantly lower than the experimental data.

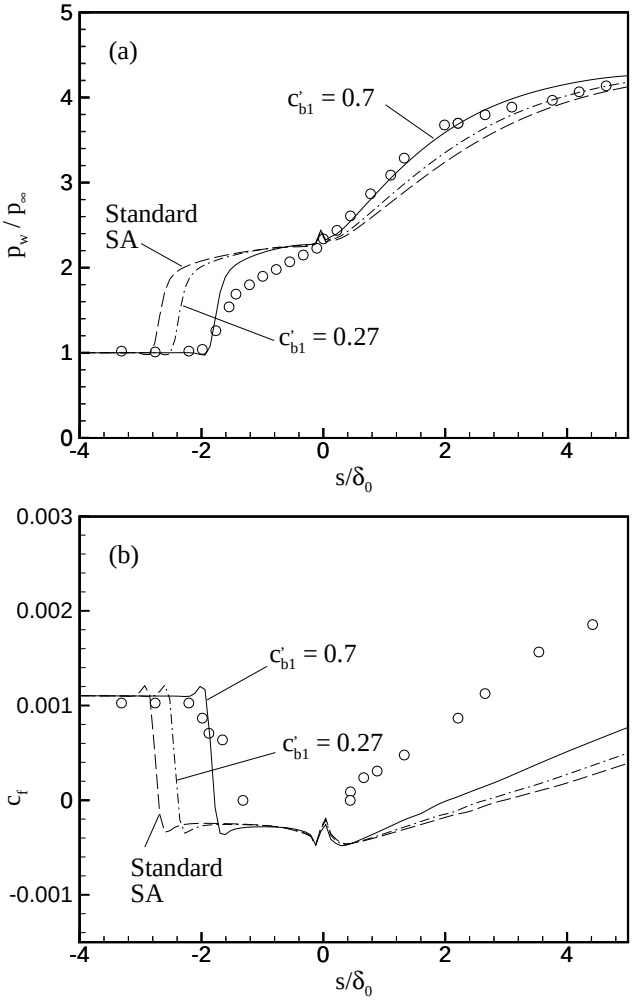

Figure 10. Variation of (a) normalized surface pressure, and (b) skin friction coefficient along a 24° compression corner obtained using the standard and modified Spalart-Allmaras models.

Conclusions

In this paper, we generalize the shock-unsteadiness modification proposed by Sinha *et al.*[7] and apply it to k-ϵ, k-ω and Spalart-Allmaras turbulence models. The effect of the correction is evaluated in flows involving shock-wave/turbulent boundary layer interaction. Compression-corner flows with three deflection angles, namely, 24°, 20°, and 16°, are considered for which experimental data is provided by Settles and Dodson.[11] Standard k-ϵ and k-ω models predict later separation in these flows than the experiments which may be caused by excessive amplification of the turbulent kinetic energy, k, through the separation shock. The shock-unsteadiness modification damps the amplification of k through the shock and results in earlier separation that matches experimental data better than the standard models. Also, the effect of the correction is found to decrease with the deflection angle such that it does not alter the separation location over low ramp angles where the standard models perform satisfactorily. However, the correction delays reattachment and results in an overly slow recovery of the boundary layer on the ramp. In the Spalart-Allmaras model, the modification amplifies eddy viscosity across the shock that moves the separation location closer to the experiment. Both the standard and modified SA models yield low values of skin friction coefficient on the ramp. Thus, while there remain some differences with experimental data, the proposed correction noticeably improves model predictions.

Acknowledgments

We would like to acknowledge the support from the Air Force Office of Scientific Research under grant F49620-01-1-0060. This work was also sponsored by the Army High Performance Computing Research Center under the auspices of the Department of the Army, Army Research Laboratory cooperative agreement number DAAD191-01-2-0014, the content of which does not necessarily reflect the position or the policy of the government, and no official endorsement should be inferred. A portion of the computer time was provided by the University of Minnesota Supercomputing Institute.

References

[1] Knight, D., Yan, H., Panaras, A., and Zheltovodov, A., "RTO WG 10: CFD Validation for Shock Wave Turbulent Boundary Layer Interactions," AIAA Paper 2002-0437, Jan. 2002.

[2] Liou, W.W., Huang, G., and Shih, T-H., "Turbulence Model Assessment for Shock Wave/Turbulent Boundary Layer Interaction in Transonic and Supersonic Flows," *Computers and Fluids*, Vol. 29, 2000, pp. 275-299.

[3] Forsythe, J., Hoffmann, K., and Damevin, H.-M., "An Assessment of Several Turbulence Models for Supersonic Compression Ramp Flow," AIAA Paper 98-2648, June 1998.

[4] Coakley, T.J., and Huang, P.G., "Turbulence Modeling for High Speed Flows," AIAA Paper 92-0436, Jan. 1992.

[5] Dolling, D.S.,"Unsteadiness of Shock-Induced Turbulent Separated Flows – Some Key Questions," AIAA Paper 2001-2708, June 2001.

[6] Knight, D.D., and Dregrez, G., "Shock Wave Boundary Layer Interactions in High Mach Number Flows – A Critical Survey of Current Numerical Prediction Capabilities," AGARD Advisory Report- 319, Vol. 11, 1998, pp. 1.1-1.35.

[7] Sinha, K., Mahesh, K., and Candler, G.V., "Modeling Shock Unsteadiness in Shock/ Turbulence Interaction," *Phys. of Fluids*, Vol. 15, No. 8, 2003, pp. 2290-2297.

[8] Launder, B.E., and Sharma, B.I., "Application of the Energy Dissipation Model of Turbulence to the Calculation of Flow near a Spinning Disc," *Letters Heat and Mass Transfer*, Vol. 1, No. 2, 1974, pp. 131-138.

[9] Sarkar, S., Erlebacher, G., Hussaini, M.Y., and Kreiss, H.O., "The Analysis and Modelling of Dilatational Terms in Compressible Turbulence," *J. Fluid Mech.*, Vol. 227, 1991, pp. 473.

[10] Sarkar, S., "The Pressure-dilatation Correlation in Compressible Flows," *Phys. Fluids A*, Vol. 4, 1992, pp. 2674-2682.

[11] Settles, G.S., and Dodson, L.J., "Supersonic and Hypersonic Shock/Boundary Layer Interaction Database," *AIAA Journal*, Vol. 32, No. 7, 1994, pp. 1377-1383.

[12] Wilcox, D.C., *Turbulence modeling for CFD*, DCW Industries, Inc., La Canada, CA, 1998, pp. 236.

[13] Wilcox, D.C., "Reassessment of the Scale Determining Equation for Advanced Turbulence Models," *AIAA Journal*, Vol. 26, No. 11, 1988, pp. 1299-1310.

[14] Spalart, P.R., and Allmaras, S.R., "A One-Equation Turbulence Model for Aerodynamic Flows," AIAA Paper 92-0439, Jan. 1992.

[15] Wilcox, D.C., "Supersonic Compression-Corner Applications of a Multiscale Model for Turbulent Flows," *AIAA Journal*, Vol. 28, No. 7, 1990, pp. 1194-1198.

[16] MacCormack, R. W. and Candler, G. V., "The Solution of the Navier-Stokes Equations Using Gauss-Seidel Line Relaxation," *Computers and Fluids,* Vol. 17, No. 1, 1989, pp. 135-150.

[17] Sinha, K. and Candler, G.V., "An Accurate Implicit Formulation of a Two-Equation Turbulence Model," AIAA Paper 98-2649, June 1998.

[18] Wright, M. J., Candler, G. V., and Bose, D., "Data-Parallel Line Relaxation Method for the Navier-Stokes Equations," *AIAA Journal,* Vol. 36, No. 9, 1998, pp. 1603-1609.

[19] Menter, F.R., "Two-Equation Eddy Viscosity Turbulence Models for Engineering Applications," *AIAA Journal*, Vol. 32, No. 8, 1994, pp. 1598-1605.

[20] Durbin, P.A., "On the k-3 stagnation point anomaly," *Int. J. of Heat Fluid Flow*, Vol. 17, 1996, pp. 89-90.

[21] F. Thivet, F., Knight, D.D., Zheltovodov, A.A., and Maksimov, A.I., "Importance of limiting the turbulent stresses to predict 3D shock-wave / boundary-layer interactions," 23rd International Symposium on Shock Waves, Fort Worth, TX, Paper No. 2761, 2001.

[22] Shih, T.H., Liou, W.W., Shabbir, A., Yang, Z., and Zhu,J., "A new $k-\epsilon$ eddy viscosity model for high Reynolds number turbulent flows," *Comput. Fluids*, Vol. 24, No. 3, 1997, pp. 227-238.